Cancer Research

Intratumoral Heterogeneity in *EGFR*-Mutant NSCLC Results in Divergent Resistance Mechanisms in Response to EGFR Tyrosine Kinase Inhibition

Margaret Soucheray[1], Marzia Capelletti[2,3,4], Inés Pulido[5], Yanan Kuang[2,3], Cloud P. Paweletz[2,3], Jeffrey H. Becker[1], Eiki Kikuchi[6], Chunxiao Xu[2], Tarun B. Patel[1], Fatima Al-shahrour[7], Julián Carretero[5], Kwok-Kin Wong[2,3,4,8], Pasi A. Jänne[2,3,4], Geoffrey I. Shapiro[2,9], and Takeshi Shimamura[1]

Abstract

Non–small cell lung cancers (NSCLC) that have developed resistance to EGF receptor (EGFR) tyrosine kinase inhibitor (TKI), including gefitinib and erlotinib, are clinically linked to an epithelial-to-mesenchymal transition (EMT) phenotype. Here, we examined whether modulating EMT maintains the responsiveness of *EGFR*-mutated NSCLCs to EGFR TKI therapy. Using human NSCLC cell lines harboring mutated *EGFR* and a transgenic mouse model of lung cancer driven by mutant *EGFR* (*EGFR-Del19-T790M*), we demonstrate that EGFR inhibition induces TGFβ secretion followed by SMAD pathway activation, an event that promotes EMT. Chronic exposure of *EGFR*-mutated NSCLC cells to TGFβ was sufficient to induce EMT and resistance to EGFR TKI treatment. Furthermore, NSCLC HCC4006 cells with acquired resistance to gefitinib were characterized by a mesenchymal phenotype and displayed a higher prevalence of the *EGFR* T790M mutated allele. Notably, combined inhibition of EGFR and the TGFβ receptor in HCC4006 cells prevented EMT but was not sufficient to prevent acquired gefitinib resistance because of an increased emergence of the *EGFR* T790M allele compared with cells treated with gefitinib alone. Conversely, another independent NSCLC cell line, PC9, reproducibly developed *EGFR* T790M mutations as the primary mechanism underlying EGFR TKI resistance, even though the prevalence of the mutant allele was lower than that in HCC4006 cells. Thus, our findings underscore heterogeneity within NSCLC cells lines harboring EGFR kinase domain mutations that give rise to divergent resistance mechanisms in response to treatment and anticipate the complexity of EMT suppression as a therapeutic strategy. *Cancer Res; 75(20); 4372–83. ©2015 AACR.*

Introduction

Activating EGF receptor (*EGFR*) mutations dictate responsiveness of non–small cell lung cancers (NSCLC) to reversible EGFR tyrosine kinase inhibitors (TKIs), including gefitinib and erlotinib (1–4). Despite promising initial responses, acquired resistance universally develops, mediated by the emergence of the secondary T790M mutation or by focal amplification of *MET*, in approximately 60% and 5% of patients, respectively (5–10).

NSCLCs with acquired EGFR TKI resistance that present with an epithelial-to-mesenchymal transition (EMT) phenotype have been identified in recent clinical studies (9, 11–13). Similarly, NSCLC cells with EGFR TKI sensitizing mutations may develop an EMT phenotype upon chronic exposure to erlotinib (14–16). EMT is a cellular program observed in normal development and is implicated in tumor progression and metastasis (17). Overexpression of the receptor tyrosine kinase (RTK) AXL has been associated with the EMT gene signature in NSCLC and confers acquired erlotinib resistance in cell line models (15, 16). AXL has therefore been proposed as a therapeutic target in EGFR TKI–resistant NSCLC cell lines with EMT phenotype. However, in other studies, AXL inhibition has not sensitized resistant cells with EMT phenotype to EGFR TKIs (18). These conflicting results suggest that

[1]Department of Molecular Pharmacology and Therapeutics, Oncology Research Institute, Loyola University Chicago, Stritch School of Medicine, Maywood, Illinois. [2]Department of Medical Oncology, Dana-Farber Cancer Institute, Boston, Massachusetts. [3]Belfer Institute for Applied Cancer Science, Dana-Farber Cancer Institute, Boston, Massachusetts. [4]Lowe Center for Thoracic Oncology, Dana-Farber Cancer Institute, Boston, Massachusetts. [5]Departament de Fisiologia, Facultat de Farmacia, Universitat de Valencia, Burjassot, Spain. [6]First department of Medicine, Hokkaido University Hospital, Sapporo, Hokkaido, Japan. [7]Translational Bioinformatics Unit, Clinical Research Programme, Spanish National Cancer Research Centre, Madrid, Spain. [8]Ludwig Center at Dana-Farber/Harvard Cancer Center, Dana-Farber Cancer Institute, Boston, Massachusetts. [9]Early Drug Development Center; Dana-Farber Cancer Institute, Boston, Massachusetts.

Note: Supplementary data for this article are available at Cancer Research Online (http://cancerres.aacrjournals.org/).

M. Soucheray and M. Capelletti contributed equally to this article.

Corresponding Author: Takeshi Shimamura, Department of Molecular Pharmacology and Therapeutics, Oncology Research Institute, Loyola University Chicago, Stritch School of Medicine, 2160 S 1st Avenue, Cardinal Bernardin Cancer Center 205, Maywood IL 60153. Phone: 708-327-3250; Fax: 708-327-3238; E-mail: tashimamura@luc.edu

doi: 10.1158/0008-5472.CAN-15-0377

AACR

developing targeted therapies for NSCLCs that have acquired EGFR TKI resistance via EMT could potentially be difficult and that a more complete understanding of the mechanisms by which the inhibition of mutant EGFR in NSCLC cells promotes EMT is required.

The study of resistance to EGFR TKIs in *EGFR*-mutated NSCLC is complex because tumor heterogeneity may promote different mechanisms of resistance at different metastatic sites (18). For example, EGFR TKI resistance with *MET* amplification may occur with or without a T790M mutation, and the occurrence varies among postmortem samples obtained from metastatic sites from the same patient (19, 20). In this regard, it is important to preclinically investigate whether *EGFR*-mutated NSCLC can remain sensitive to EGFR TKIs by successfully suppressing EMT or whether the acquisition of divergent resistance mechanisms will limit the use of this strategy.

To elucidate the mechanisms promoting EMT in NSCLCs harboring mutated *EGFR*, we have performed analyses using multiplex growth factor and cytokine assays and genomic signatures of NSCLC cells in which acquired EGFR TKI resistance is associated with the EMT phenotype. We have also evaluated the ability of combined EGFR inhibition and EMT suppression to prevent acquired resistance and have investigated the significance of tumor heterogeneity in NSCLC in the emergence of EGFR TKI acquired resistance.

Materials and Methods

NSCLC cell lines and STR assays

HCC827, HCC4006, and NCI-H1975 NSCLC cells were obtained from the ATCC and were maintained as specified. The cell lines were tested by certified third-party laboratories for authenticity (Fig. 5B and Supplementary Materials and Methods). Details for the STR assay are described in the Supplementary Methods. gDNA from PC9 was used extensively in previous studies and its authenticity has been confirmed (21, 22).

Generation of EGFR TKI or gefitinib/SB431542-resistant cells

To generate cell lines resistant to first-generation EGFR TKIs, HCC4006 or HCC827 cells were exposed to increasing concentrations of gefitinib or erlotinib over 6 months in a manner similar to previously described (22–24); however, resulting resistant cell lines for HCC4006 cells are polyclonal and not clones. Gefitinib/SB431542-resistant HCC4006 cells were developed in a similar manner, with continuous exposure to 1 μmol/L SB431542. For HCC827 erlotinib–resistant cells, clones were isolated. All resistant cells are able to proliferate normally in the presence of 10 μmol/L gefitinib. Cell viability was used to confirm gefitinib resistance after allowing the cells to grow gefitinib-free for 7 days. Upon confirming resistance, cells were cultured without drugs and their resistance to gefitinib was examined periodically.

Generation of EGFR TKI–resistant cells by TGFβ1 exposure

HCC827 and HCC4006 cells were grown in RPMI-1640 supplemented with FBS and 10 ng/mL of human recombinant TGFβ1 (Life). Cells were seeded at 70% confluence in 60-mm dishes and the media were replaced every other day until cells started proliferating normally (28–30 days).

Cell viability assays and cell counting

NSCLC cells were cultured in the presence of drugs or vehicle for 72 hours, and viability was determined using the Cell Counting Kit-8 (CCK-8) colorimetric assay (Dojindo) as previously described (25). The results were analyzed and displayed using Prism 6 (GraphPad Software). Equal amounts of cells were seeded in the assays to compare cell growth kinetics. Live cells were counted using Countess (Life). Details are provided in the Supplementary Methods.

Western blot analysis

Lysate preparation and Western blotting were performed as described previously (26). A list of antibodies used is available in the Supplementary Methods.

Luminex assay

Details for Luminex-based multibead assays are available in the Supplementary Methods.

shRNA constructs and lentiviral infection

pLKO.1 shRNA constructs designed by The RNAi Consortium were used as described previously (26). shRNA sequences and procedures are provided in the Supplementary Methods.

RNA and DNA extraction

RNA from cell lines was extracted and purified using QIAshredder and RNeasy Plus (Qiagen) according to the manufacturer's instructions. DNA was extracted using the DNeasy Blood and Tissue Kit (Qiagen). DNA and RNA samples were quantified using NanoDrop ND-2000 Spectrophotometer (ThermoScientific) followed by Qubit (Life).

DNA sequencing

EGFR exons 19 and 20 were amplified from DNA from cell lines using primers described previously (27). Resulting PCR products were purified and subjected to Sanger sequencing (Genewiz). Primer sequences and conditions are available in the Supplementary Methods.

Detection of *EGFR* T790M with ddPCR

Droplet digital PCR (ddPCR) was performed at the Belfer Institute, Dana-Farber Cancer Institute (Boston, MA), as previously described (28).

Analysis of microarray gene expression data

Gene expression profiling methods are available in the Supplementary Methods.

Detection of apoptosis by flow cytometry

Adherent cells were removed from plates using Accutase (Life) and pooled. Apoptosis was assessed using an Annexin V-FLUOS Staining Kit (Roche) according to the manufacturer's instructions.

Murine drug treatment studies

Human EGFR exon 19 deletion/T790M (TD)-inducible bitransgenic mice were generated and have been previously characterized (24). After continuous exposure to doxycycline diets for more than 8 weeks, bitransgenic mice were subjected to MRI to document the lung tumor burden. After initial imaging, mice were treated either with vehicle (10% 1-methyl-2-pyrrolidinone:90% PEG-300) alone or WZ4002, the mutant-selective EGFR TKI with activity against T790M, at 25 mg/kg gavage daily.

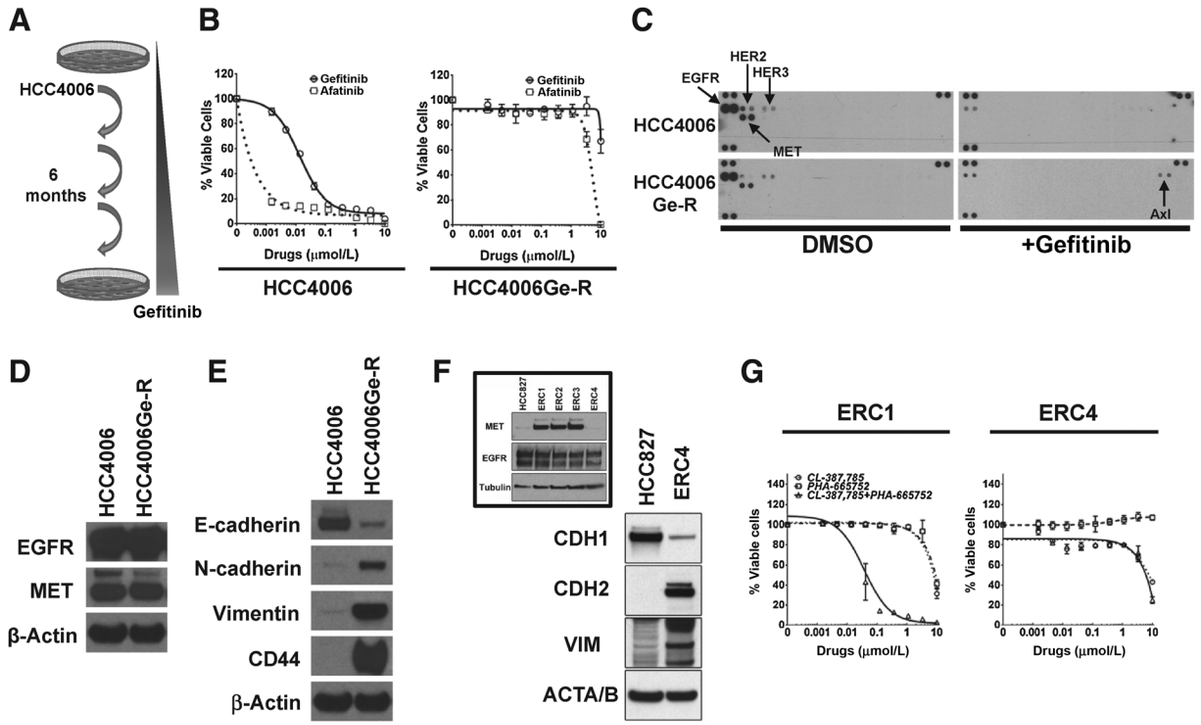

Figure 1.
EGFR TKI–resistant cells with a mesenchymal phenotype develop as mass culture or single subclone. A, EGFR-mutant human NSCLC cell line HCC4006 was made resistant to gefitinib by growing it in increasing concentrations of gefitinib for 6 months. B, parental HCC4006 and mass culture of resistant HCC4006Ge-R cells were treated with gefitinib or afatinib at the indicated concentrations for 72 hours and viable cells were quantified. The percentage of viable cells is shown relative to untreated controls. Data points are average of duplicate wells from two independent assays. Error bars, SD. C, phospho-RTK array reveals that HCC4006Ge-R cells maintain little phosphorylation of EGFR and AXL in the presence of 10 μmol/L gefitinib. Duplicate spots in the corners are phospho-tyrosine controls. D, no apparent overexpression of EGFR or MET was detected in HCC4006Ge-R cells. E, HCC4006Ge-R cells show upregulation of canonical mesenchymal markers and downregulation of epithelial markers. F, inset, Western blot analysis shows that majority of EGFR TKI–resistant clones overexpress MET upon chronic exposure of HCC827 cells to erlotinib. A subclone #4 (ERC4) shows no MET overexpression, whereas canonical mesenchymal markers are upregulated (right). G, 72-hours cell viability assay with EGFR inhibitor (CL-387,785) or MET inhibitor (PHA-665752) or a combination. Note ERC4 is resistant to the combination treatment. Data points are average of duplicate wells from two independent assays. Error bars, SD.

Histology and immunohistochemistry

After sacrifice, the left lung of each mouse was dissected and snap-frozen for biochemical analysis. The right lung was inflated with buffered 10% formalin for 10 minutes and fixed in 10% formalin overnight at room temperature. The specimen was washed once in PBS, placed in 70% ethanol, and embedded in paraffin, from which 5-μm sections were generated. IHC was performed in the Department of Pathology at Brigham and Women's Hospital (Boston, MA). A list of antibodies used is available in the Supplementary Methods.

Statistical analysis

Unless otherwise stated, comparisons of statistical significance were performed using the Student *t* test. $P < 0.05$ was considered statistically significant.

Results

Chronic exposure of *EGFR*-mutated NSCLC cells to increasing concentrations of gefitinib promotes acquired EGFR TKI resistance with a mesenchymal phenotype

We first generated a mass culture of HCC4006 cells that were resistant to gefitinib (HCC4006Ge-R) by growing cells in increasing concentrations of gefitinib to a final concentration of 10 μmol/L for up to 6 months *in vitro* (Fig. 1A). Cell viability and Annexin V apoptosis assays confirmed that HCC4006Ge-R cells (Ge-R) are highly resistant to gefitinib and afatinib compared with the parental HCC4006 cells (Fig. 1B, Supplementary Fig. S1A). RTK profiling revealed that EGFR, MET, HER2, and HER3 are tyrosine-phosphorylated in Ge-R cells cultured without gefitinib. Prolonged exposure of Ge-R cells to gefitinib suppressed RTK phosphorylation, except for residual phosphorylation of EGFR and AXL (Fig. 1C). However, the treatment of Ge-R cells with the combination of gefitinib and the AXL inhibitor R428 failed to decrease the viability of Ge-R cells (Supplementary Fig. S1B). The levels of EGFR and MET expression are comparable in HCC4006 and Ge-R cells (Fig. 1D). The morphology of Ge-R cells is characteristic of that observed in mesenchymal cells. Western blotting using antibodies against canonical epithelial and mesenchymal markers revealed that Ge-R cells underwent EMT (Fig. 1E). Similarly, NCI-H1975 (H1975) cells harboring L858R/T790M grown resistant to the irreversible EGFR TKI, CL-387,785 (Supplementary Fig. S1C) also demonstrated a mesenchymal phenotype (Supplementary Fig. S1D).

In contrast, chronic EGFR inhibition in HCC827 cells predominantly resulted in erlotinib-resistant cells with *MET* amplification. Subcloning was required to isolate erlotinib-resistant

HCC827 cells demonstrating a mesenchymal phenotype without evidence of *MET* amplification (Fig. 1F). The mesenchymal clone (ERC4) was resistant to combined EGFR and MET inhibition (Fig. 1G). Gene set enrichment analysis (GSEA) demonstrated that ERC4 cells are mesenchymal with significant gene set enrichment for a gefitinib resistance signature (Supplementary Fig. S1E).

In summary, the mass culture of HCC4006 or H1975 cells grown resistant to reversible and irreversible EGFR TKIs, respectively, were mesenchymal, whereas subcloning was necessary to isolate erlotinib-resistant HCC827 cells that are mesenchymal. These experiments demonstrate that the probability of EMT emerging as a mechanism of EGFR TKI resistance varies among *EGFR*-mutated NSCLC cell lines.

TGFβ1 promotes EMT and EGFR TKI resistance that is reversible

Using Luminex-based multiplex assays, we profiled growth factors and cytokines in the supernatants from erlotinib-resistant HCC827 cell clones (Fig. 2A). In the mesenchymal ERC4 clone, TGFβ1 was the most abundant growth factor secreted, whereas it was less abundant in *MET*-amplified clones. In 2 of 3 MET-amplified clones, increased HGF secretion was observed, suggesting the presence of a MET–HGF autocrine loop, as previously reported (8). The amount of TGFβ1 secreted from HCC4006Ge-R cells was also significantly greater than that from parental HCC4006 cells (Fig. 2B, $P = 0.0084$). On the basis of the results, we hypothesized that TGFβ1-mediated mesenchymal transition makes mutant EGFR NSCLC cells resistant to EGFR TKIs. To test the hypothesis, we chronically exposed HCC827 cells to 10 ng/mL of TGFβ1 for 30 days. This promoted a mesenchymal phenotype. In addition, removal of TGFβ1 from the cell culture media for more than 30 days partially restored an epithelial phenotype (Fig. 2C). HCC827 cells were resistant to EGFR TKIs in the TGFβ1-induced mesenchymal state, and the removal of TGFβ1 restored sensitivity (Fig. 2D). Surprisingly, TGFβ1-mediated mesenchymal transition was associated with a significant reduction in ERBB family receptor expression (Fig. 2E), even though the cells were able to proliferate normally. Similarly, exposure of HCC4006 cells to TGFβ1 also promoted mesenchymal transition and EGFR TKI resistance, which was reversible upon removal of TGFβ1 from the media (Supplementary Fig. S2A).

Erlotinib treatment of HCC827 cells results in dephosphorylation of AKT and ERK and induction of the proapoptotic protein BIM, as shown previously (29). In contrast, erlotinib treatment of HCC827 TGFβ1 cells failed to suppress phosphorylation of EGFR, AKT, and ERK or to induce BIM (Fig. 2F). Similarly, treatment of HCC4006 cells with 10 ng/mL of TGFβ1 for 30 days promoted a mesenchymal phenotype (Supplementary Fig. S2B) and a 100-fold increase in resistance to gefitinib when compared with parental HCC4006 cells (Supplementary Fig. S2C). These results demonstrate that continued exposure to TGFβ1 is necessary to maintain the mesenchymal phenotype and EGFR TKI–resistant state.

Chronic EGFR inhibition promotes secretion of TGFβ1 and subsequent activation of the SMAD pathway

We next investigated whether chronic EGFR inhibition was sufficient to promote continuous TGFβ1 secretion. Supernatants from HCC4006 cells treated with 100 nmol/L gefitinib were collected at 24, 48, and 72 hours. TGFβ1 concentration in the cell-free supernatants was measured by Luminex-based assay and normalized using the number of live cells attached to the plate at the time of harvest. TGFβ1 secreted by the surviving cells significantly increased over time (Fig. 3A). Similarly, TGFβ1 secretion from HCC827 cells was profoundly increased upon EGFR TKI treatment (Supplementary Fig. S3A). Equimolar erlotinib and gefitinib equally promoted TGFβ1 secretion from HCC827 or HCC4006 cells (Supplementary Fig. S3B). In contrast, EGFR wild-type NCI-H1734 cells did not demonstrate a statistically significant increase in TGFβ1 secretion after EGFR TKI exposure.

To test whether the secreted TGFβ1 is biologically active and able to stimulate TGFβ receptors expressed on HCC827 cells, the phosphorylation status of TGFβ receptor downstream proteins, SMAD2 and SMAD3, was monitored using the multiplex Luminex assay. Increased phosphorylation of SMAD2 (S465/467) and SMAD3 (S423/425) correlated with the increased secretion of TGFβ, and the phosphorylation was significantly downregulated in the presence of the TGFβ receptor inhibitor SB431542 (Fig. 3B). Western blotting confirmed that HCC4006 cells treated with erlotinib show increased SMAD2 (S465/467) phosphorylation, despite a decrease in total SMAD2 protein expression and that phosphorylation was diminished in the presence of SB431542 (Supplementary Fig. S3C). Consistent with the insignificant increase of TGFβ secretion in EGFR wild-type (WT) cells, erlotinib treatment of NCI-H1734 cells failed to induce phosphorylation of SMAD2 and SMAD3 (Supplementary Fig. S3D).

To extend our findings to *in vivo*, we assessed whether similar events occurred in mouse lung cancers driven by human *EGFR* exon19 deletion/T790M (TD) that respond to the EGFR mutant–specific irreversible TKI WZ4002 to promote tumor regression (24). Treatment of the mouse tumors with WZ4002 for 2 days suppressed EGFR activity and activated SMAD2/3 activities, recapitulating our finding in cell lines (Fig. 3C).

To eliminate the possibility that off-target effects of erlotinib are responsible for the induction of TGFβ1 secretion, we used target-specific shRNA-mediated depletion of *EGFR* in HCC827 cells. Upon puromycin selection, clones with MET overexpression or EMT were isolated (Supplementary Fig. S3E) similar to clones isolated in the erlotinib-resistant population (Fig. 1F). Slight *MET* amplification was observed in clone 10 but not in clone 9 (Supplementary Fig. S3F). Clone 9 was resistant to gefitinib (Fig. 3E) without apparent upregulation of RTKs (Supplementary Fig. S3G). GSEA revealed significant enrichment of mesenchymal and gefitinib-resistant gene signatures in this clone (Fig. 3F) and demonstrated a marked increase in TGFβ1 secretion (Fig. 3G, $P = 0.0011$) albeit after prolonged EGFR knockdown.

Concurrent EGFR and TGFβR inhibition prevents mesenchymal transition but does not avert emergence of EGFR TKI resistance

We next investigated whether cotreatment with an EGFR inhibitor and a TGFβ receptor inhibitor is effective in preventing the emergence of EMT-mediated EGFR TKI resistance in these cells. HCC4006 cells were grown in the presence of gefitinib or gefitinib and SB431542 for 6 months (Fig. 4A) until they demonstrated normal growth kinetics in the presence of increasing inhibitor concentrations. Lysates from cells cultured more than 3 months in the presence of drugs were subjected to Western blotting with the indicated antibodies (Fig. 4B). HCC4006 cells continuously treated with gefitinib alone exhibited reduced expression of the epithelial marker E-cadherin and an increased level of the mesenchymal marker vimentin (Fig. 4B). In HCC4006 cells cotreated

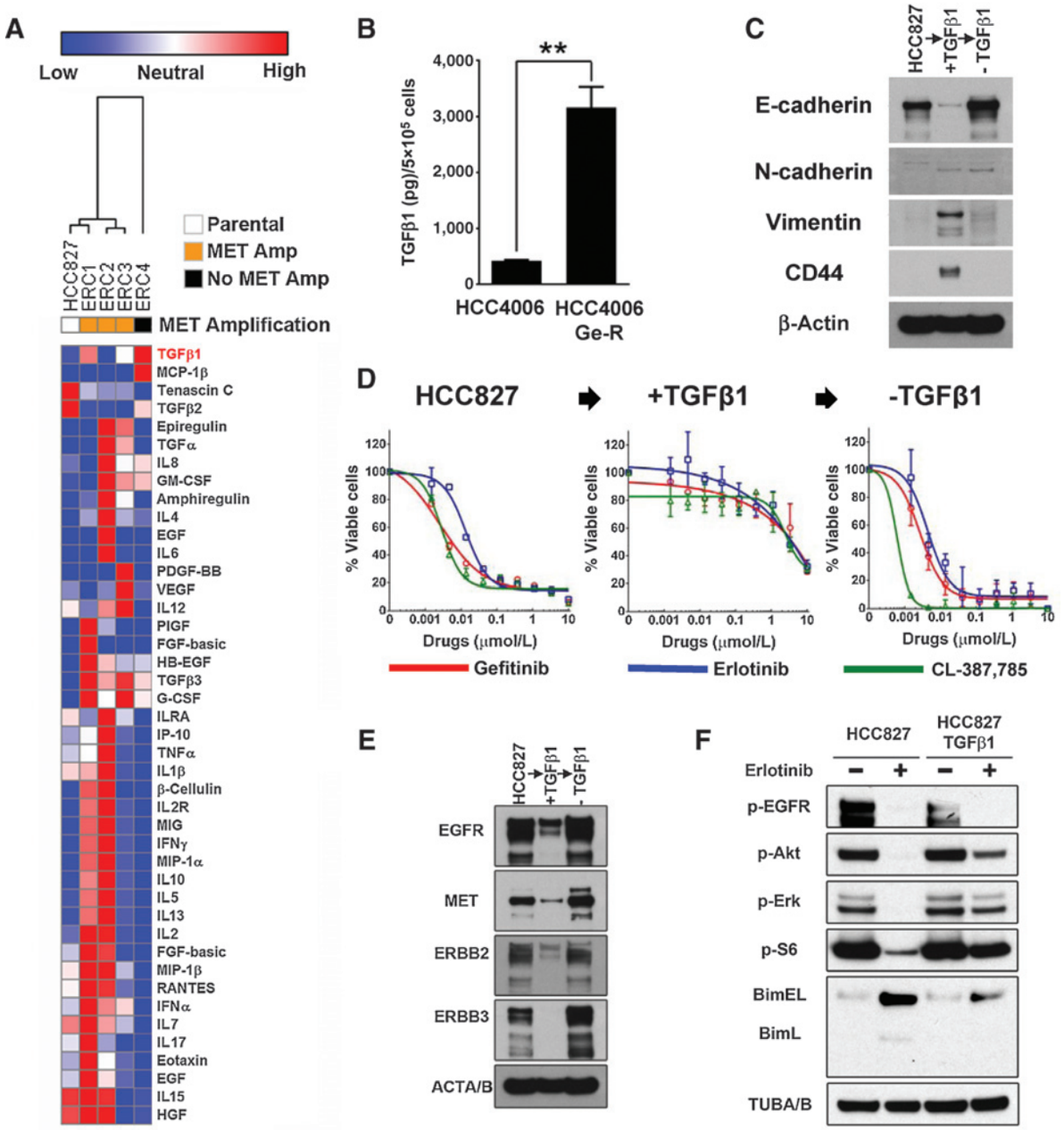

Figure 2.
EMT in HCC827 and HCC4006 cells is promoted by TGFβ1. A, heatmap showing relative amount of each growth factor and cytokine secreted from HCC827 erlotinib–resistant clones. Concentrations of growth factor (pg/mL) were $\log_2$-transformed, and relative amount for each growth factor and cytokines was displayed using a heatmap. B, bar graph illustrating significantly increased TGFβ1 secretion in HCC4006Ge-R. Differences between parental and HCC4006Ge-R cells (**, $P = 0.0084$) were calculated by the Student t test. C, immunoblot demonstrating changes in E-cadherin, vimentin, N-cadherin, and CD44 expression upon TGFβ1 (10 ng/mL) treatment of HCC827 cells for >30 days and TGFβ1 removal for >30 days. D, the 72-hour cell viability assay demonstrating the effect of EGFR TKIs in HCC827 cells that are TGFβ1-naïve, TGFβ1 treated for >30 days, and TGFβ1 removed >30 days. Data points are average of duplicate wells from two independent assays. Error bars, SD. E, immunoblot showing the expression of ERBB receptors upon exposure to and removal of TGFβ1. F, immunoblot showing how secondary signaling molecules and proapoptotic molecule Bim respond to erlotinib treatment, whereas HCC827 cells are in epithelial state without TGFβ1 exposure (HCC827) and in mesenchymal state with TGFβ1 exposure (HCC827 TGFβ1).

with gefitinib and SB431592, E-cadherin and vimentin levels were largely unchanged. SMAD2 phosphorylation, indicative of TGFβ pathway activation, was not observed after cotreatment with gefitinib and SB431592. EGFR phosphorylation was significantly suppressed in HCC4006 cells treated with gefitinib alone; however, gefitinib failed to inhibit EGFR phosphorylation in

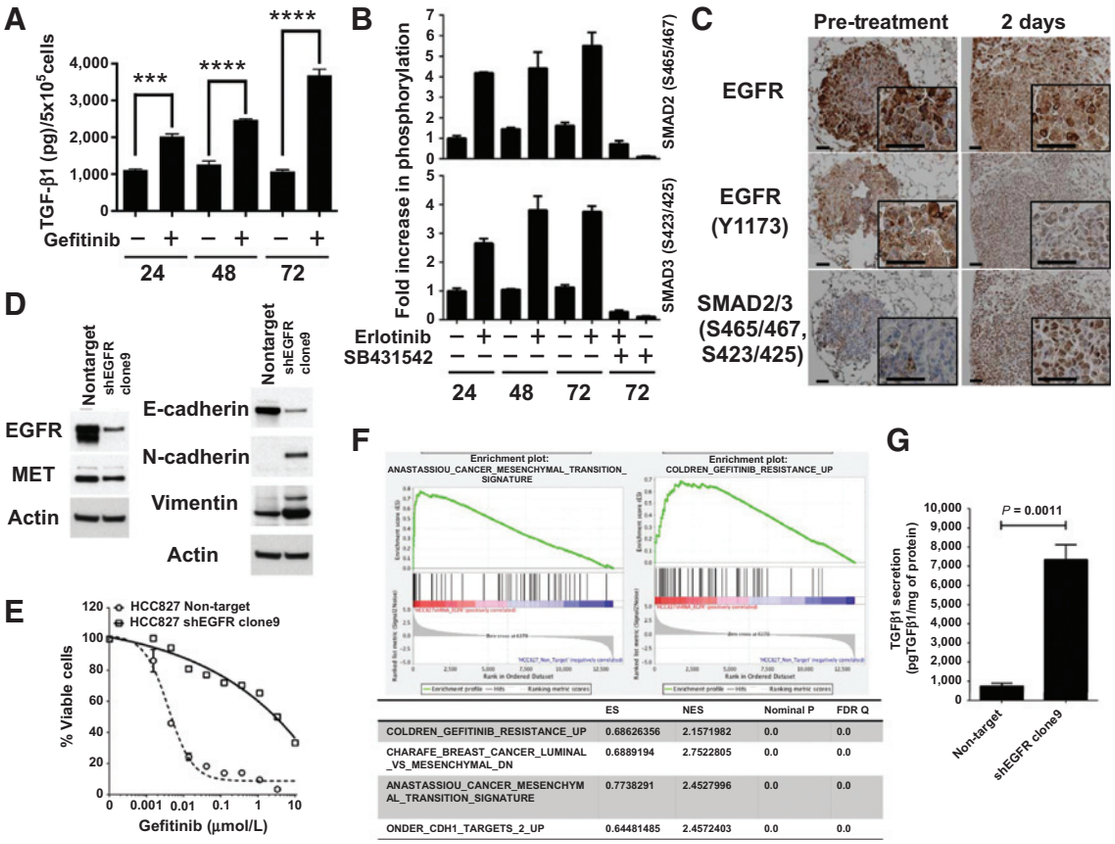

	ES	NES	Nominal P	FDR Q
COLDREN_GEFITINIB_RESISTANCE_UP	0.68626356	2.1571982	0.0	0.0
CHARAFE_BREAST_CANCER_LUMINAL_VS_MESENCHYMAL_DN	0.6889194	2.7522805	0.0	0.0
ANASTASSIOU_CANCER_MESENCHYMAL_TRANSITION_SIGNATURE	0.7738291	2.4527996	0.0	0.0
ONDER_CDH1_TARGETS_2_UP	0.64481485	2.4572403	0.0	0.0

Figure 3.
EGFR inhibition in EGFR-mutant cells promotes secretion of TGFβ1 to stimulate TGFβ–SMAD axis. A, erlotinib-treated HCC4006 cells secrete TGFβ1 into the media in a time-dependent manner. The concentration of TGFβ1 in the media was normalized to 5×10^5 cells. *, $P < 0.05$; **, $P < 0.01$; ***, $P < 0.001$. B, HCC4006 cells were treated with DMSO, erlotinib (100 nmol/L), SB431542 (1 μmol/L), or combination of erlotinib and SB431542 for 72 hours. Viable cells were lysed and equal amounts of protein were subjected to a Luminex assay to quantify the SMAD2 and SMAD3 activities. Fold increase of phosphorylated proteins was calculated using mean fluorescent intensity that was proportional to the amount of phosphorylated protein in the cell. The results represent an average of two independent assays run in duplicate samples. −, DMSO treatment; +, drug treatment. Error bars, SD. C, IHC staining of EGFR T790M/Del19 lung tumors shows that WZ4002 treatment suppresses EGFR activity while increasing SMAD2/3 activities. IHC for EGFR (top) and phosphorylated EGFR at tyrosine 1173 and phosphorylated SMAD2 and 3 at S465/467 and S423/425 sites, respectively (bottom). Photos shown are representative fields in each group in low and high magnification. Scale bars, 50 μm. D, Western blot analyses showing the efficiency of EGFR knockdown and upregulation of mesenchymal markers. HCC827 shEGFR clone9 with constitutive EGFR knockdown by lentiviral shRNA (shEGFR clone 9). HCC827 cells were transduced with lentiviral shRNA coding for nontarget shRNA and serve as a control (Nontarget). Twenty micrograms of lysates was subject to Western blotting with indicated antibodies. Representative blots from more than three independent experiments are shown. E, 72-hour cell viability assay reveals that shEGFR#9 cells confer gefitinib resistance. Data points are average of duplicate wells from two independent assays. Error bars, SD. F, GSEA of shEGFR#9 cells. The normalized enrichment score (NES) and the nominal *P* values are indicated. G, TGFβ1 secretion is significantly ($P = 0.00011$) increased in HCC827shEGFR#9 (Student *t* test).

HCC4006 cells cotreated with gefitinib and SB431592 toward the end of the treatment (Fig. 4B). Interestingly, culturing HCC827 cells in increasing concentrations of gefitinib resulted in the initial depletion of E-cadherin and increase of N-cadherin and vimentin over the first 24 days (Supplementary Fig. S4A); however, long-term (6 month) incubation predominantly gave rise to gefitinib-resistant cells with *MET* amplification (data not shown).

GeSB-R cells harbor T790M mutation and remain modestly sensitive to AZD9291

At the end of 6-month treatment, HCC4006 cells proliferate normally in the presence of 10 μmol/L gefitinib (Ge-R) with a mesenchymal phenotype or in the presence of 10 μmol/L gefitinib and 1 μmol/L SB431542 (GeSB-R) with an epithelial phenotype (Supplementary Fig. S4B). Because gefitinib failed to inhibit EGFR in GeSB-R, we challenged the resulting cells with the irreversible EGFR inhibitor, afatinib (Fig. 4C). While gefitinib failed to inhibit EGFR in GeSB-R cells, afatinib dephosphorylated EGFR in GeSB-R. Despite the complete inhibition of EGFR by gefitinib and afatinib in GeR cells, downstream AKT and ERK phosphorylation persisted, suggesting the presence of a bypass pathway to activate downstream signaling (Fig. 4D). In GeSB-R cells, afatinib but not gefitinib reduced AKT and ERK phosphorylation. GeR cells were resistant to both gefitinib and afatinib, whereas GeSB-R remained fairly sensitive to afatinib. Afatinib treatment induced a small degree of apoptosis in GeSB-R cells (Supplementary Fig. S4C).

We extracted DNA from HCC4006, Ge-R, and GeSB-R cells and performed sequencing of EGFR. Sanger sequencing demonstrated that both Ge-R and GeSB-R cells preserved c.2239_3348delinsC *EGFR* deletion mutation in exon 19; however, a secondary T790M

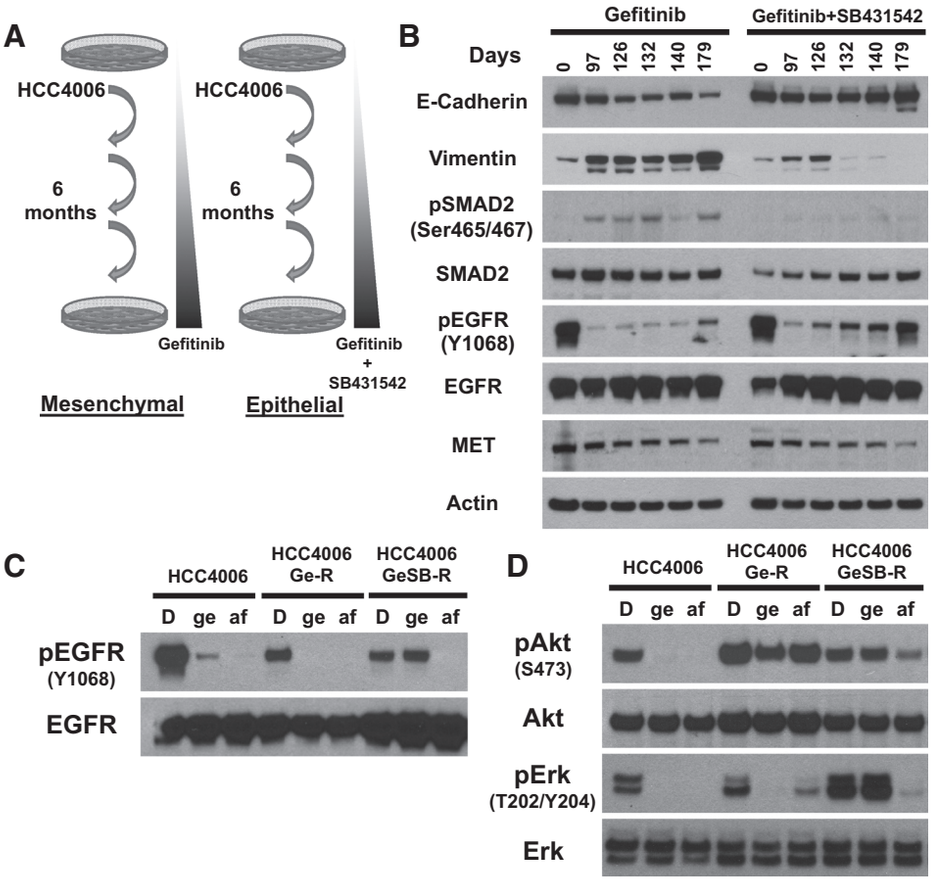

Figure 4.
Concurrent EGFR and TGFβR inhibition prevents mesenchymal transition but does not avert emergence of EGFR TKI resistance. A, EGFR-mutant HCC4006 human NSCLC cell line was grown in increasing concentrations of gefitinib with or without SB431542 for 6 months. B, immunoblotting showing the persisting SMAD2 activation and mesenchymal transition in HCC4006 cells treated with gefitinib over the course of 3 to 6 months. The presence of SB431542 prevents mesenchymal transition induced by continuous gefitinib treatment in HCC4006 cells. Lysates were made at indicated times and they were subjected to Western blotting with antibodies indicated. C, immunoblots showing that afatinib but not gefitinib dephosphorylated EGFR in HCC4006GeSB-R cells. HCC4006 and HCC4006 grown resistant to gefitinib (HCC4006Ge-R) and to gefitinib in the presence of SB431542 (HCC4006GeSB-R) were treated with DMSO (D), 500 nmol/L gefitinib (ge), or 500 nmol/L afatinib (af) for 24 hours. Lysates were made and subjected to Western blotting with antibodies indicated. D, same lysates prepared in C were subjected to immunoblots showing signaling molecules downstream of EGFR.

mutation in exon 20 of the *EGFR* gene was only detected in GeSB-R cells (Fig. 5A). DNA samples were next subjected to ddPCR assays that have been used to detect rare mutations (30). The prevalence of EGFR T790M mutation detected was highest in GeSB-R cells (18.3%) and was significantly lower in Ge-R cells (1.2%; Fig. 5B).

AZD9291 is a potent and selective third-generation EGFR irreversible inhibitor that has been shown to potently inhibit EGFR with T790M (31, 32). On the basis of sequencing and ddPCR results, we challenged HCC4006, Ge-R, and GeSB-R cells with DMSO or 500 nmol/L of AZD9291 for 2 hours (Supplementary Fig. S5A). AZD9291 depleted EGFR phosphorylation in HCC4006, Ge-R, and GeSB-R cells; however, complete dephosphorylation of downstream secondary signaling molecules, AKT, ERK, and S6, was only evident in HCC4006 cells. Residual AKT, ERK, and S6 phosphorylation was evident in GeSB-R cells treated with AZD9291. Consistent with the phosphorylation status of AKT, ERK, and S6 phosphorylation in parental, Ge-R, and GeSB-R HCC4006 cells, parental cells were most sensitive and Ge-R cells were most resistant to AZD9291 (Supplementary Fig. S5B).

Preexisting T790M mutation is more abundant in HCC4006 cells than in PC9 cells

Previous reports suggested that the T790M mutation pre-exists *in cis* with a primary EGFR-activating mutation in a small population and is positively selected upon EGFR TKI treatment (22, 23, 33). PC9 cells are well characterized to reproducibly develop EGFR TKI resistance via the emergence of T790M (18, 34). In contrast, the prevalence of T790M in gefitinib-resistant HCC4006 cells (Ge-R) was fairly low (1.2%), and the impact of T790M in gefitinib resistance was not evident unless HCC4006 cells were cotreated with gefitinib and SB431542 (GeSB-R). Consequently, we tried to estimate the prevalence of preexisting cell population with T790M both in PC9 and in HCC4006. We performed ddPCR using a high number of replicates [250000 Genome Equivalent (GE) in 48 wells] to evaluate the relative frequency of T790M allele compared with wild-type T790 allele (Fig. 6A). We were able to identify the presence of T790M allele in both the parental cell lines investigated with a frequency of 0.0738% in HCC4006 cells and of 0.0360% in PC9 cells.

To verify that Ge-R and GeSB-R were derived from parental HCC4006 cells, we performed 16 point STR cell authentication on parental HCC4006, HCC4006Ge-R with a mesenchymal phenotype, and HCC4006GeSB-R cells (Supplementary Fig. S6B). D16S539 STR on chromosome 11 was missing in HCC4006Ge-R cells, whereas HCC4006GeSB-R cells maintain D16S539 STR on chromosomes 11 and 12. D3S1358 STR on chromosome 18 was missing in HCC4006GeSB-R cells, whereas HCC4006GeR cells carry D3S1358 STR on chromosomes 16 and 18. Interestingly, Ge-R and GeSB-R cells differ by 2 STRs, but the combined STR profile of the 2 resistant cell populations perfectly matches the STR profile of HCC4006 cells. This result suggests that the parental HCC4006 cell line is heterogeneous and minimally contains 2 discrete subpopulations of cells with different STR profiles. Each of the 2 subpopulations was selected in response to a different selection pressure.

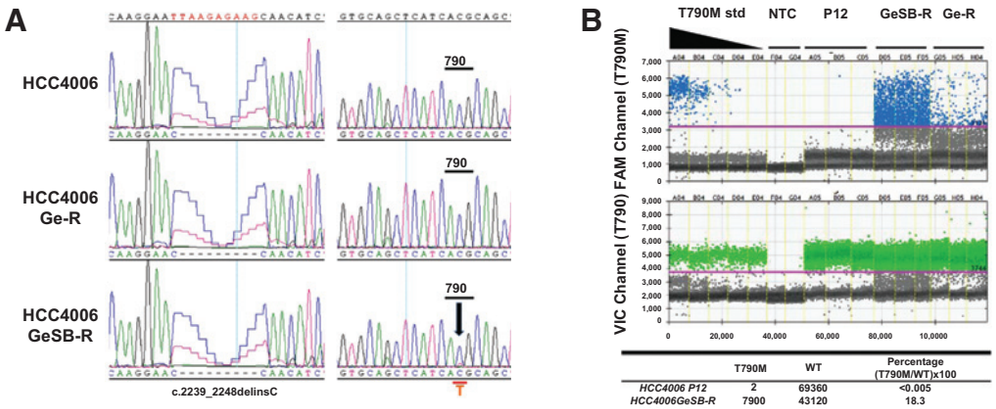

C

HCC4006Ge-R

	HCC4006 Ge-R	HCC4006 ATCC
D3S1358	16, 18	
D7S820	9, 12	9, 12
vWa	16, 17	16, 17
FGA	21, 22	
D8S1179	10, 14	
D21S11	31	
D18S51	19	
D5S818	12	12
D13S317	11, 12	11, 12
D16S539	12	11, 12
TH01	7	7
TPOX	8, 9	8, 9
CSF1PO	10	10
AMEL	X	X
Penta D	9, 14	
Penta E	7, 13	
% Match to ATCC profile	93%	N/A
% Match to parental	96%	

HCC4006

	HCC4006 Parental	HCC4006 ATCC
D3S1358	16, 18	
D7S820	9, 12	9, 12
vWa	16, 17	16, 17
FGA	21, 22	
D8S1179	10, 14	
D21S11	31	
D18S51	19	
D5S818	12	12
D13S317	11, 12	11, 12
D16S539	11, 12	11, 12
TH01	7	7
TPOX	8, 9	8, 9
CSF1PO	10	10
AMEL	X	X
Penta D	9, 14	
Penta E	7, 13	
% Match to ATCC profile	100%	N/A
% Match to parental	N/A	100%

HCC4006GeSB-R

	HCC4006 GeSB-R	HCC4006 ATCC
D3S1358	16	
D7S820	9, 12	9, 12
vWa	16, 17	16, 17
FGA	21, 22	
D8S1179	10, 14	
D21S11	31	
D18S51	19	
D5S818	12	12
D13S317	11, 12	11, 12
D16S539	11, 12	11, 12
TH01	7	7
TPOX	8, 9	8, 9
CSF1PO	10	10
AMEL	X	X
Penta D	9, 14	
Penta E	7, 13	
% Match to ATCC profile	100%	N/A
% Match to parental	96%	

Figure 5.
Suppression of gefitinib-induced EMT in HCC4006 preferentially selects for cells with acquired T790M mutation. A, DNA sequence analysis of exons 19 and 20 of the EGFR gene in HCC4006, HCC4006Ge-R, and HCC4006GeSB-R cells showing the presence of c. 2239_2248delinsC (p. L747_A750delinsP) deletion mutation. Electropherograms show T790M mutation of the EGFR gene only in HCC4006GeSB-R cells. B, ddPCR quantification of allelic prevalence of EGFR T790M versus total EGFR (T790) in HCC4006, HCC4006Ge-R, and HCC4006GeSB-R cells. C, authentication of HCC4006, HCC4006Ge-R, and HCC4006GeSB-R cells by 16 points STR demonstrates that different subpopulations of HCC4006 cells were selected by the different treatments.

Discussion

Several groups have reported histologic changes in NSCLC specimens obtained from tumors with acquired EGFR TKI resistance that are consistent with EMT (9, 12, 13). However, the molecular mechanisms underlying EMT and their impact on the etiology of EGFR TKI resistance have not been fully elucidated.

Using EGFR TKIs and shRNA targeting EGFR, we have shown that EGFR inhibition or depletion promotes TGFβ1 secretion from both the EGFR-mutant HCC827 and HCC4006 cell lines (Fig. 3A and G). However, it remains unclear how EGFR inhibition results in TGFβ secretion in *EGFR*-mutated cells. It has been reported that erlotinib- resistant PC9 cells promote TGFβ2 secretion with enhanced motility, although the resistant cells do not exhibit a mesenchymal phenotype (35). It is possible that the TGFβ species secreted following EGFR inhibition is cell lineage–specific. Nonetheless, in HCC827 and HCC4006 cells, the increase in TGFβ1 secretion correlated with the activation of downstream SMAD targets *in vitro* and *in vivo* (Fig. 3B and C), and the presence of TGFβ receptor inhibitor, SB431542, attenuated SMAD activation *in vitro*. Of note, erlotinib treatment of NCI-H1734 cells harboring wild-type *EGFR* did not promote significant TGFβ1 secretion (Supplementary Fig. S3A) or SMAD activation (Supplementary Fig. S3D). These results suggest that inhibition of mutated-*EGFR* establishes the autocrine TGFβ1 pathway loop to positively stimulate the SMAD pathway in *EGFR*-mutant NSCLC.

Several studies have demonstrated that exposing *EGFR*-mutant NSCLC cells to TGFβ1 induces EMT associated with EGFR TKI resistance (14, 36, 37). However, it is unclear whether the EGFR TKI resistance was due to cytostatic effects mediated by TGFβ1, as slow-growing tumors are inherently resistant to therapies (38). We have cultured EGFR-mutant HCC827 and HCC4006 cells in the presence of 10 ng/mL TGFβ1 until they achieved a mesenchymal state and proliferated at the same rate as parental cells (Supplementary Fig. S2D). The mesenchymal cells are resistant to EGFR TKIs and lose expression of ERBB receptors while they maintain downstream pathways critical for proliferation and survival (Fig. 2F). Despite the phosphorylation of EGFR and AXL that was demonstrated on RTK arrays, mesenchymal Ge-R cells did not appear to depend on major RTK oncogenic drivers for growth and survival, as concurrent EGFR and AXL inhibition

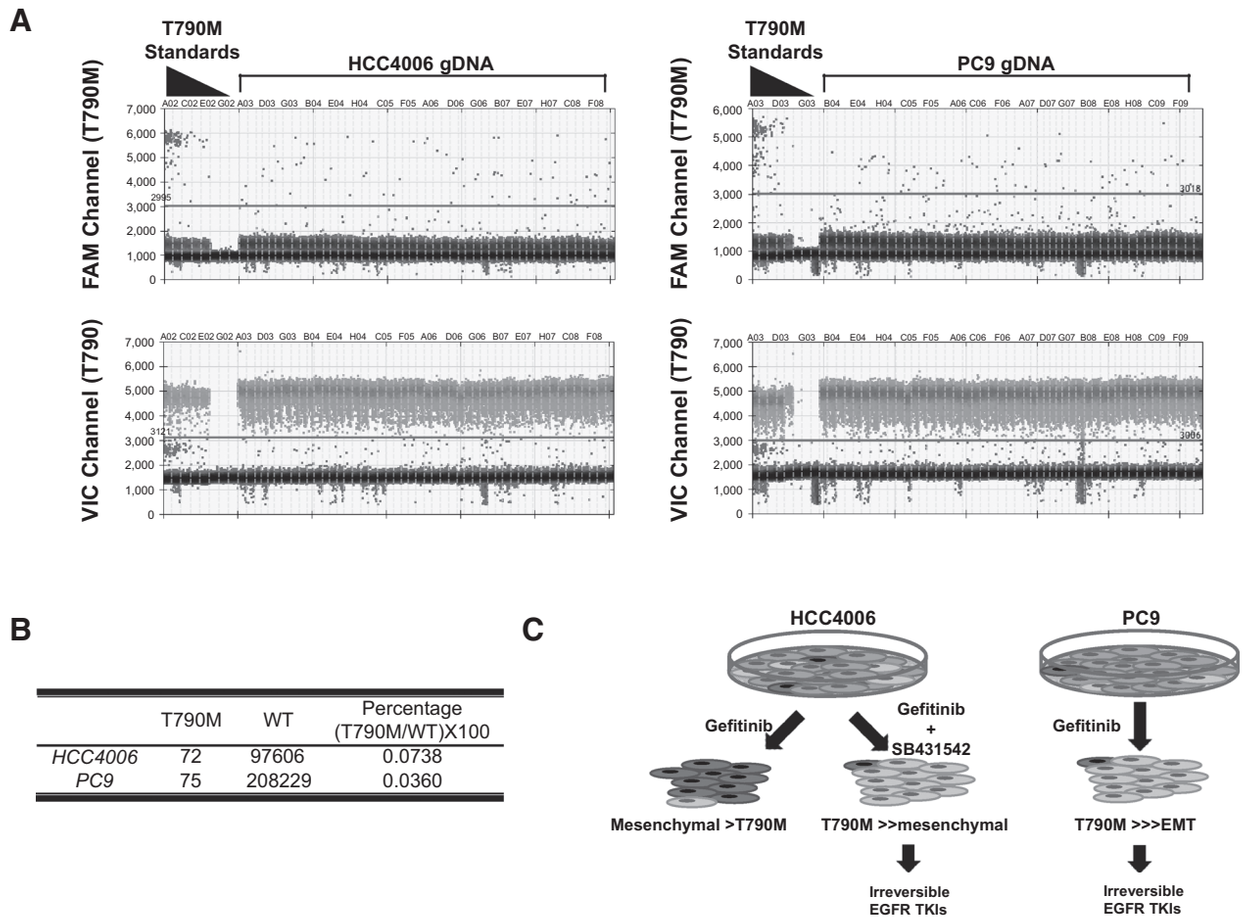

	T790M	WT	Percentage (T790M/WT)X100
HCC4006	72	97606	0.0738
PC9	75	208229	0.0360

Figure 6.
A subset of HCC4006 harbors *EGFR* T790M mutation prior to drug treatments. A, ddPCR quantification of the allelic prevalence of EGFR T790M versus total EGFR (T790) in HCC4006 cells (left) and PC9 cells (right). Two hundred and fifty thousand genomic equivalent were used in 48 wells. B, frequency of T790M mutant allele in HCC4006 cells and PC9 cells. C, schematic representation of resistant mechanisms in NSCLC cells harboring EGFR kinase domain mutation upon EGFR TKI and EGFR TKI/TGFβ receptor inhibitor cotreatment.

failed to kill the resistant cells (Supplementary Fig. S1B). These results strongly suggest the presence of novel oncogenic drivers in EGFR TKI–resistant NSCLC with EMT.

TGFβ1-induced mesenchymal transition and EGFR TKI resistance in HCC827 and HCC4006 cells were reversible upon TGFβ1 withdrawal (Fig. 2C and D). Chronic exposure of EGFR-mutant NSCLC to EGFR inhibitors underlies the establishment of a continuous TGFβ1 autocrine loop and subsequent EMT-mediated EGFR TKI resistance. Taken together, our results suggest that sustained TGFβ secretion following chronic EGFR inhibition provides a suitable environment for EGFR-mutant NSCLC cells to undergo EMT. It is noteworthy that patients with NSCLC who progressed on an EGFR TKI therapy responded to the treatment after a "drug holiday" (39, 40); however, it remains unclear how the discontinuation of the therapy resensitizes the EGFR-mutant NSCLC to EGFR inhibition. Our experimental results suggest that relieving EGFR inhibition could deplete TGFβ1 to reverse EMT, which in turn might resensitize tumors to EGFR TKIs, thus prolonging the duration of EGFR TKI therapy. However, the fact that the mesenchymal phenotype and TKI resistance in HCC827 (ERC4) and HCC4006Ge-R is irreversible after TGFβ receptor inhibition suggests that approaches to reverse EMT may only be plausible as a preventive strategy.

In HCC4006 cells, combined EGFR and TGFβ inhibition successfully prevented gefitinib-induced EMT; however, the resulting cells still became resistant to gefitinib, and the population was enriched with cells that harbor EGFR secondary T790M mutation (18.3%, Fig. 5B). To date, EGFR TKI resistance via emergence of a T790M secondary mutation has not been reported in HCC4006 cells. Of note, the irreversible EGFR TKI, AZD9291, dephosphorylated EGFR in GeSB-R cells; however, complete dephosphorylation of downstream secondary signaling molecules, AKT, ERK, and S6, was only evident in parental HCC4006 cells, not in GeSB-R (Supplementary Fig. S5A). This result suggests the presence of a heterogeneous population in GeSB-R cells and also suggests that the use of third-generation mutant-selective EGFR TKIs that inhibit T790M might be attenuated in cells composed of a heterogeneous population.

Whether the resistance mechanisms to EGFR TKIs evolve under the selective pressure of the drugs or preexist prior to treatment is the subject of ongoing investigation. Here, we performed ddPCR-based T790M detection in HCC4006 cells and in PC9 cells and

found a small subpopulation of the cells harboring T790M mutant allele in both cell lines with frequencies of 0.0738% and 0.0360%, respectively (Fig. 6B). Despite the low frequency of T790M alleles in parental PC9 cells, PC9 cells reproducibly develop resistance to reversible EGFR TKIs with T790M secondary mutation (34, 41). In contrast, HCC4006 cells, with a slightly greater frequency of T790M alleles, reproducibly develop TKI resistance with a mesenchymal phenotype. This finding suggests that the prevalence of T790M alleles in parental cells does not necessarily predict the emergence of EGFR TKI resistance with T790M. The fact that the frequency of T790M alleles in HCC4006Ge-R (Fig. 5B, 1.2%) was much lower than the frequency in HCC4006GeSB-R suggests that heterogeneous tumors inherently possess the potential to give rise to EGFR TKI–resistant cells with different resistance mechanisms depending on the treatment (Fig. 6C). Our results from STR analysis also support the notion that the cells with a discrete genetic makeup are selected by a particular treatment regimen from the heterogeneous cell population. Taken together, our results highlight the difficulty in interpreting results from functional assays that use human NSCLC cell lines harboring *EGFR* mutation, as we need to account for tumor heterogeneity within the cell population.

This view is further supported by our original observation that the abundance of TGFβ1 in the growth media following EGFR inhibition does not preferentially select for the emergence of EMT-associated EGFR TKI resistance. Despite the fact that prolonged EGFR inhibition in HCC827 cells provides a favorable environment for the cells to undergo EMT with an increase in TGFβ1 concentration, the cells predominantly develop EGFR TKI resistance through *MET* amplification. Only a limited subpopulation of the clones develops EMT-mediated EGFR TKI resistance (Fig. 1F). In contrast, HCC4006 cells reproducibly develop EMT-associated EGFR TKI resistance (Fig. 1B; ref. 14).

In HCC4006 cells concurrently treated with gefitinib and SB431542, the mesenchymal marker vimentin initially increased and then decreased (Fig. 4B). This phenomenon could be explained by heterogeneity in HCC4006 cells. HCC4006 cells have a propensity to develop EGFR TKI resistance with EMT (14, 36, 42, 43); thus, the cells with mesenchymal phenotype and high vimentin initially remain in the culture. However, the presence of SB431542 does not allow other epithelial cells to engage in mesenchymal transition. As a result, a subset of HCC4006 cells harboring EGFR secondary T790M with an epithelial phenotype eventually dominate in the culture.

While we have demonstrated that TGFβ1-induced mesenchymal transition and EGFR TKI resistance in EGFR-mutated NSCLC cells are reversible, mesenchymal transition and EGFR TKI resistance in HCC4006GeR and HCC827 ERC4 cells were not reversible with chronic exposure to SB431542 (data not shown). These results suggest that either EGFR TKI–resistant subpopulations with a mesenchymal phenotype preexist in the parental population or that 6 months of EGFR TKI treatment results in irreversible changes in *EGFR*-mutated NSCLC cells. These points will require further clarification. Moreover, oncogenic drivers in EGFR TKI resistant cells with a mesenchymal phenotype must be discovered to formulate a strategy to overcome the resistance.

In conclusion, we found that an increase in TGFβ concentration induced by the inhibition of mutant EGFR is complicit in the development of EGFR TKI resistance associated with EMT. Our results suggest that the combination of TGFβ and EGFR targeted therapies is efficacious in preventing the emergence of EMT-associated EGFR TKI resistance in EGFR-mutant NSCLC cells. However, combination treatment did not prevent the emergence of EGFR TKI resistance in EGFR-mutant HCC4006 cells but rather provided a suitable environment for the rare subset of cells harboring T790M mutation to emerge. Despite the presence of the T790M subpopulation, HCC4006 cells reproducibly develop resistance to reversible EGFR TKIs by undergoing EMT. This finding suggests that the detection of T790M in primary tumors prior to reversible EGFR TKI treatment may not necessarily predict the emergence of acquired resistance with secondary EGFR T790M mutation. Our current findings also provide insight into how selection pressure by drug treatments underlies the etiology of EGFR TKI resistance grown out of heterogeneous EGFR-mutant NSCLC cell populations.

Disclosure of Potential Conflicts of Interest

P.A. Jänne reports receiving commercial research grant from AstraZeneca and Astellas; has ownership interest (including patents) from Gatekeeper Pharmaceuticals; is a consultant/advisory board member of AstraZeneca, Pfizer, Clovis Oncology, and Roche; and has provided expert testimony for Labcorp. No potential conflicts of interest were disclosed by the other authors.

Authors' Contributions

Conception and design: M. Soucheray, M. Capelletti, J. Carretero, K.-K. Wong, G.I. Shapiro, T. Shimamura

Development of methodology: M. Soucheray, M. Capelletti, Y. Kuang, K.-K. Wong, T. Shimamura

Acquisition of data (provided animals, acquired and managed patients, provided facilities, etc.): M. Soucheray, M. Capelletti, I. Pulido, Y. Kuang, C.P. Paweletz, J.H. Becker, E. Kikuchi, C. Xu, J. Carretero, P.A. Jänne, G.I. Shapiro, T. Shimamura

Analysis and interpretation of data (e.g., statistical analysis, biostatistics, computational analysis): M. Soucheray, M. Capelletti, I. Pulido, Y. Kuang, J.H. Becker, E. Kikuchi, F. Al-shahrour, J. Carretero, G.I. Shapiro, T. Shimamura

Writing, review, and/or revision of the manuscript: M. Soucheray, M. Capelletti, Y. Kuang, C.P. Paweletz, J.H. Becker, T.B. Patel, J. Carretero, P.A. Jänne, G.I. Shapiro, T. Shimamura

Administrative, technical, or material support (i.e., reporting or organizing data, constructing databases): M. Soucheray, C. Xu, G.I. Shapiro, T. Shimamura

Study supervision: K.-K. Wong, G.I. Shapiro, T. Shimamura

Acknowledgments

The authors thank Drs. Rick Wiese, Debra MacIvor, and Joseph Hwang at Millipore for providing invaluable technical assistance for Milliplex Luminex assays and Patricia Simms and Ashley Hess at Loyola University Chicago Stritch School of Medicine, Flow Cytometry Core Facility.

Grant Support

This work is initiated with the support from Claudia Adams Barr Program in Innovative Basic Cancer Research at Dana-Farber Cancer Institute (T. Shimamura and G.I. Shapiro) and is supported by American Cancer Society Illinois Division Basic Science Grant #254563 and Loyola University Chicago Program Development Funding (T. Shimamura). This work is also supported by research fellowship from Sumitomo Life Social Welfare Services Foundation (E. Kikuchi), MINECO (SAF2010-21769), ISCIII (RD12/0036/0045) and Generalitat Valenciana (ACOMP/2013/156 and ACIF/2013/239; J. Carretero), NIH grants CA140594, CA122794, CA163896, CA166480 (K.-K. Wong), CA114465, CA135257, and CA154303 (P.A. Jänne).

The costs of publication of this article were defrayed in part by the payment of page charges. This article must therefore be hereby marked *advertisement* in accordance with 18 U.S.C. Section 1734 solely to indicate this fact.

Received February 5, 2015; revised May 21, 2015; accepted July 2, 2015; published OnlineFirst August 17, 2015.

References

1. Lynch TJ, Bell DW, Sordella R, Gurubhagavatula S, Okimoto RA, Brannigan BW, et al. Activating mutations in the epidermal growth factor receptor underlying responsiveness of non-small-cell lung cancer to gefitinib. N Engl J Med 2004;350:2129–39.
2. Paez JG, Janne PA, Lee JC, Tracy S, Greulich H, Gabriel S, et al. EGFR mutations in lung cancer: correlation with clinical response to gefitinib therapy. Science 2004;304:1497–500.
3. Sordella R, Bell DW, Haber DA, Settleman J. Gefitinib-sensitizing EGFR mutations in lung cancer activate anti-apoptotic pathways. Science 2004;305:1163–7.
4. Pao W, Miller V, Zakowski M, Doherty J, Politi K, Sarkaria I, et al. EGF receptor gene mutations are common in lung cancers from "never smokers" and are associated with sensitivity of tumors to gefitinib and erlotinib. Proc Natl Acad Sci U S A 2004;101:13306–11.
5. Engelman JA, Zejnullahu K, Mitsudomi T, Song Y, Hyland C, Park JO, et al. MET amplification leads to gefitinib resistance in lung cancer by activating ERBB3 signaling. Science 2007;316:1039–43.
6. Kobayashi S, Boggon TJ, Dayaram T, Janne PA, Kocher O, Meyerson M, et al. EGFR mutation and resistance of non-small-cell lung cancer to gefitinib. N Engl J Med 2005;352:786–92.
7. Kobayashi S, Ji H, Yuza Y, Meyerson M, Wong KK, Tenen DG, et al. An alternative inhibitor overcomes resistance caused by a mutation of the epidermal growth factor receptor. Cancer Res 2005;65: 7096–101.
8. Turke AB, Zejnullahu K, Wu YL, Song Y, Dias-Santagata D, Lifshits E, et al. Preexistence and clonal selection of MET amplification in EGFR mutant NSCLC. Cancer Cell 2010;17:77–88.
9. Sequist LV, Waltman BA, Dias-Santagata D, Digumarthy S, Turke AB, Fidias P, et al. Genotypic and histological evolution of lung cancers acquiring resistance to EGFR inhibitors. Sci Transl Med 2011;3:75ra26.
10. Yu HA, Arcila ME, Rekhtman N, Sima CS, Zakowski MF, Pao W, et al. Analysis of tumor specimens at the time of acquired resistance to EGFR-TKI therapy in 155 patients with EGFR-mutant lung cancers. Clin Cancer Res 2013;19:2240–7.
11. Crystal AS, Shaw AT, Sequist LV, Friboulet L, Niederst MJ, Lockerman EL, et al. Patient-derived models of acquired resistance can identify effective drug combinations for cancer. Science 2014;346: 1480–6.
12. Uramoto H, Iwata T, Onitsuka T, Shimokawa H, Hanagiri T, Oyama T. Epithelial-mesenchymal transition in EGFR-TKI acquired resistant lung adenocarcinoma. Anticancer Res 2010;30:2513–7.
13. Chung JH, Rho JK, Xu X, Lee JS, Yoon HI, Lee CT, et al. Clinical and molecular evidences of epithelial to mesenchymal transition in acquired resistance to EGFR-TKIs. Lung Cancer 2011;73: 176–82.
14. Suda K, Tomizawa K, Fujii M, Murakami H, Osada H, Maehara Y, et al. Epithelial to mesenchymal transition in an epidermal growth factor receptor-mutant lung cancer cell line with acquired resistance to erlotinib. J Thorac Oncol 2011;6:1152–61.
15. Byers LA, Diao L, Wang J, Saintigny P, Girard L, Peyton M, et al. An epithelial-mesenchymal transition gene signature predicts resistance to EGFR and PI3K inhibitors and identifies Axl as a therapeutic target for overcoming EGFR inhibitor resistance. Clin Cancer Res 2013;19: 279–90.
16. Zhang Z, Lee JC, Lin L, Olivas V, Au V, LaFramboise T, et al. Activation of the AXL kinase causes resistance to EGFR-targeted therapy in lung cancer. Nat Genet 2012;44:852–60.
17. Kalluri R, Weinberg RA. The basics of epithelial-mesenchymal transition. J Clin Invest 2009;119:1420–8.
18. Chong CR, Janne PA. The quest to overcome resistance to EGFR-targeted therapies in cancer. Nat Med 2013;19:1389–400.
19. Suda K, Murakami I, Katayama T, Tomizawa K, Osada H, Sekido Y, et al. Reciprocal and complementary role of MET amplification and EGFR T790M mutation in acquired resistance to kinase inhibitors in lung cancer. Clin Cancer Res 2010;16:5489–98.
20. Bean J, Brennan C, Shih JY, Riely G, Viale A, Wang L, et al. MET amplification occurs with or without T790M mutations in EGFR mutant lung tumors with acquired resistance to gefitinib or erlotinib. Proc Natl Acad Sci U S A 2007;104:20932–7.
21. Ercan D, Xu C, Yanagita M, Monast CS, Pratilas CA, Montero J, et al. Reactivation of ERK signaling causes resistance to EGFR kinase inhibitors. Cancer Discov 2012;2:934–47.
22. Ercan D, Zejnullahu K, Yonesaka K, Xiao Y, Capelletti M, Rogers A, et al. Amplification of EGFR T790M causes resistance to an irreversible EGFR inhibitor. Oncogene 2010;29:2346–56.
23. Engelman JA, Mukohara T, Zejnullahu K, Lifshits E, Borras AM, Gale CM, et al. Allelic dilution obscures detection of a biologically significant resistance mutation in EGFR-amplified lung cancer. J Clin Invest 2006; 116:2695–706.
24. Zhou W, Ercan D, Chen L, Yun CH, Li D, Capelletti M, et al. Novel mutant-selective EGFR kinase inhibitors against EGFR T790M. Nature 2009; 462:1070–4.
25. Shimamura T, Lowell AM, Engelman JA, Shapiro GI. Epidermal growth factor receptors harboring kinase domain mutations associate with the heat shock protein 90 chaperone and are destabilized following exposure to geldanamycins. Cancer Res 2005;65:6401–8.
26. Shimamura T, Li D, Ji H, Haringsma HJ, Liniker E, Borgman CL, et al. Hsp90 inhibition suppresses mutant EGFR-T790M signaling and overcomes kinase inhibitor resistance. Cancer Res 2008;68:5827–38.
27. Janne PA, Borras AM, Kuang Y, Rogers AM, Joshi VA, Liyanage H, et al. A rapid and sensitive enzymatic method for epidermal growth factor receptor mutation screening. Clin Cancer Res 2006;12:751–8.
28. Oxnard GR, Paweletz CP, Kuang Y, Mach SL, O'Connell A, Messineo MM, et al. Noninvasive detection of response and resistance in EGFR-mutant lung cancer using quantitative next-generation genotyping of cell-free plasma DNA. Clin Cancer Res 2014;20: 1698–705.
29. Deng J, Shimamura T, Perera S, Carlson NE, Cai D, Shapiro GI, et al. Proapoptotic BH3-only BCL-2 family protein BIM connects death signaling from epidermal growth factor receptor inhibition to the mitochondrion. Cancer Res 2007;67:11867–75.
30. Hindson BJ, Ness KD, Masquelier DA, Belgrader P, Heredia NJ, Makarewicz AJ, et al. High-throughput droplet digital PCR system for absolute quantitation of DNA copy number. Anal Chem 2011;83:8604–10.
31. Cross DA, Ashton SE, Ghiorghiu S, Eberlein C, Nebhan CA, Spitzler PJ, et al. AZD9291, an irreversible EGFR TKI, overcomes T790M-mediated resistance to EGFR inhibitors in lung cancer. Cancer Discov 2014;4: 1046–61.
32. Finlay MR, Anderton M, Ashton S, Ballard P, Bethel PA, Box MR, et al. Discovery of a potent and selective EGFR inhibitor (AZD9291) of both sensitizing and T790M resistance mutations that spares the wild type form of the receptor. J Med Chem 2014;57:8249–67.
33. Ogino A, Kitao H, Hirano S, Uchida A, Ishiai M, Kozuki T, et al. Emergence of epidermal growth factor receptor T790M mutation during chronic exposure to gefitinib in a non small cell lung cancer cell line. Cancer Res 2007;67:7807–14.
34. Cortot AB, Repellin CE, Shimamura T, Capelletti M, Zejnullahu K, Ercan D, et al. Resistance to irreversible EGFR tyrosine kinase inhibitors through a multistep mechanism involving the IGF1R pathway. Cancer Res 2013; 73:834–43.
35. Serizawa M, Takahashi T, Yamamoto N, Koh Y. Combined treatment with erlotinib and a transforming growth factor-beta type I receptor inhibitor effectively suppresses the enhanced motility of erlotinib-resistant non-small-cell lung cancer cells. J Thorac Oncol 2013; 8:259–69.
36. Wilson C, Ye X, Pham T, Lin E, Chan S, McNamara E, et al. AXL inhibition sensitizes mesenchymal cancer cells to antimitotic drugs. Cancer Res 2014;74:5878–90.
37. Buonato JM, Lazzara MJ. ERK1/2 blockade prevents epithelial-mesenchymal transition in lung cancer cells and promotes their sensitivity to EGFR inhibition. Cancer Res 2014;74:309–19.
38. Moore N, Houghton J, Lyle S. Slow-cycling therapy-resistant cancer cells. Stem Cells Dev 2012;21:1822–30.
39. Becker A, Crombag L, Heideman DA, Thunnissen FB, van Wijk AW, Postmus PE, et al. Retreatment with erlotinib: Regain of TKI sensitivity following a drug holiday for patients with NSCLC who initially responded to EGFR-TKI treatment. Eur J Cancer 2011; 47:2603–6.

40. Oxnard GR, Janjigian YY, Arcila ME, Sima CS, Kass SL, Riely GJ, et al. Maintained sensitivity to EGFR tyrosine kinase inhibitors in EGFR-mutant lung cancer recurring after adjuvant erlotinib or gefitinib. Clin Cancer Res 2011;17:6322–8.
41. Chmielecki J, Foo J, Oxnard GR, Hutchinson K, Ohashi K, Somwar R, et al. Optimization of dosing for EGFR-mutant non-small cell lung cancer with evolutionary cancer modeling. Sci Transl Med 2011;3:90ra59.
42. Ohashi K, Maruvka YE, Michor F, Pao W. Epidermal growth factor receptor tyrosine kinase inhibitor-resistant disease. J Clin Oncol 2013;31:1070–80.
43. Ware KE, Hinz TK, Kleczko E, Singleton KR, Marek LA, Helfrich BA, et al. A mechanism of resistance to gefitinib mediated by cellular reprogramming and the acquisition of an FGF2-FGFR1 autocrine growth loop. Oncogenesis 2013;2:e39.